

Comparisons of Radiative Transfer Models of Vegetation Canopies and Laboratory Measurements

Shunlin Liang,^{*} Alan H. Strahler,[†] Xifeng Jin,[‡] and Qijang Zhu[§]

Laboratory measurements of the directional reflectance of plant canopies fit radiative-transfer-based plane-parallel models well when the plants are low and leaves are small. Bidirectional reflectance measurements were collected at a unique facility in Changchun, China, using an apparatus that simulates solar radiation at zenith angles up to 45° on a 1-m square target. A curved arm fitted with multiband radiometers revolves on a circular track around the target, allowing rapid measurement of multispectral bidirectional reflectance factors (BRFs) of the target at 10°-zenith and azimuth angles. Because the measurements are made under controlled conditions, effects of such confounding factors as wind and diffuse (sky) irradiance can be avoided. Three one-dimensional radiative-transfer canopy models were compared to the BRF measurements in the near-infrared. The models generally fit the data for a young wheat canopy well. However, young corn and soybean canopies showed significant differences that are attributed to the escape of multiply scattered radiation from the sides of the canopy.
©Elsevier Science Inc., 1997

INTRODUCTION

In recent years, a number of mathematical models have been devised to describe the directional scattering be-

havior of leaf canopies. Beginning with the relatively simple model of Suits (1972), which assumed all leaves to be either horizontal or vertical and randomly oriented in azimuth, such models have been refined to provide highly sophisticated abstractions of the physical interactions of photon streams with vegetation covers. Approaches to modeling have varied from geometric optics (Li and Strahler, 1986; 1992), in which the vegetation canopy is taken as a collection of three-dimensional plant crowns that cast shadows on each other and on the background, to radiative transfer (Goel, 1988; Myneni et al., 1990a), in which the vegetation is taken as a volume-scattering medium of finite scattering elements. There were several experiments conducted in the field to evaluate the effects of sun-view geometry and soil on bidirectional reflectance (e.g., Ranson et al., 1985a,b; Huete and Jackson, 1988; Huete et al., 1985). Canopy reflectances were measured with different background and geometry in those experiments; similar approaches have been adapted in this study. Although a number of other measurement datasets are also available (e.g., Kimes et al., 1984; Vanderbilt and Grant, 1986; Irons et al., 1992; Deering et al., 1994), data acquisition has not kept pace with model development. Only a limited number of datasets are available that provide both radiance measurements and independent measurements of the physical parameters driving the reflectance models (e.g., Ranson et al., 1985b). Most of those measurements were made in the field.

This article describes a laboratory facility located in the People's Republic of China that provides for the acquisition of directional reflectance measurements of plant canopies under controlled conditions. As an example of the utility of such measurements, we also document datasets describing the reflectance of young wheat, corn, and soybean canopies along with their physical

^{*} Department of Geography, University of Maryland at College Park

[†] Center for Remote Sensing and Department of Geography, Boston University

[‡] Changchun Institute of Optics and Fine Mechanics, Chinese Academy of Science

[§] Department of Geography, Beijing Normal University

Address correspondence to Dr. Alan Strahler, Center for Remote Sensing, Boston University, 725 Commonwealth Ave., Boston, MA 02215.

Received 26 September 1995; revised 25 October 1996.

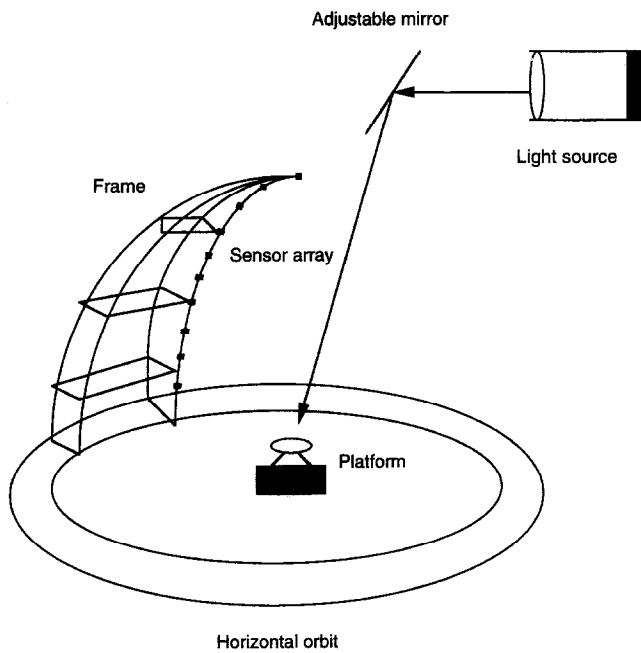


Figure 1. Illustration of the measurement apparatus in the simulation laboratory.

characteristics and use the datasets to validate three versions of a radiative-transfer style canopy reflectance model.

Laboratory measurement of directional reflectance has several distinct advantages over field measurements. First, by using a single collimated light source, irradiance can be restricted to direct beam only, eliminating the effects of diffuse radiation that are present in field measurements. Second, the effects of wind are also elimi-

Table 1. Detector Wavebands

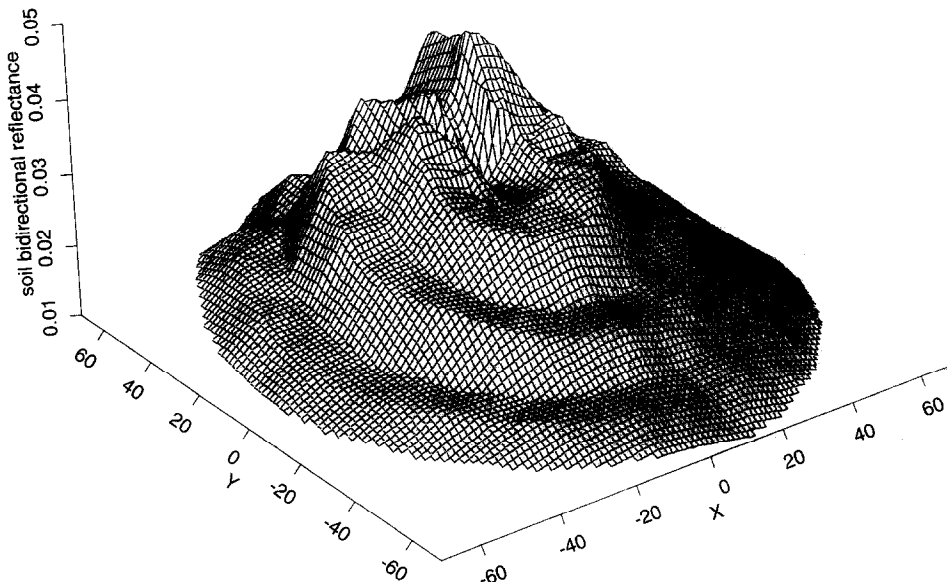
Detector	Wavelength (μm)
1	0.45–0.52
2	0.52–0.60
3	0.63–0.69
4	0.40–0.70
5	0.76–0.90
6	0.70–1.10

nated, allowing accurate measurement of leaf angle distribution. A third advantage is that the position of the source of irradiance in the hemisphere can be fixed in position. Outdoors, the sun constantly changes angular position in the sky, which may be a problem if the period of acquisition of directional radiance measurements is protracted. An important disadvantage of the laboratory approach lies primarily in that there are practical limits to the size of the target. For the facility described here, the sample stage is of 1 sq m area, and so is most suited to observations of young and/or small plants.

LABORATORY MEASUREMENTS

The directional reflectance measurements described in this paper were acquired at the Solar Simulation Laboratory for the Measurement of Bidirectional Reflectance, a facility of the Changchun Institute of Optics and Fine Mechanics, Chinese Academy of Sciences, located in the city of Changchun, Jilin Province, People’s Republic of China. The laboratory is further affiliated with the Jinguetan Remote Sensing Test Site, which is also a facility of the Chinese Academy of Science.

Figure 2. Measured bidirectional reflectance of a wet soil with the illumination angle 30°.



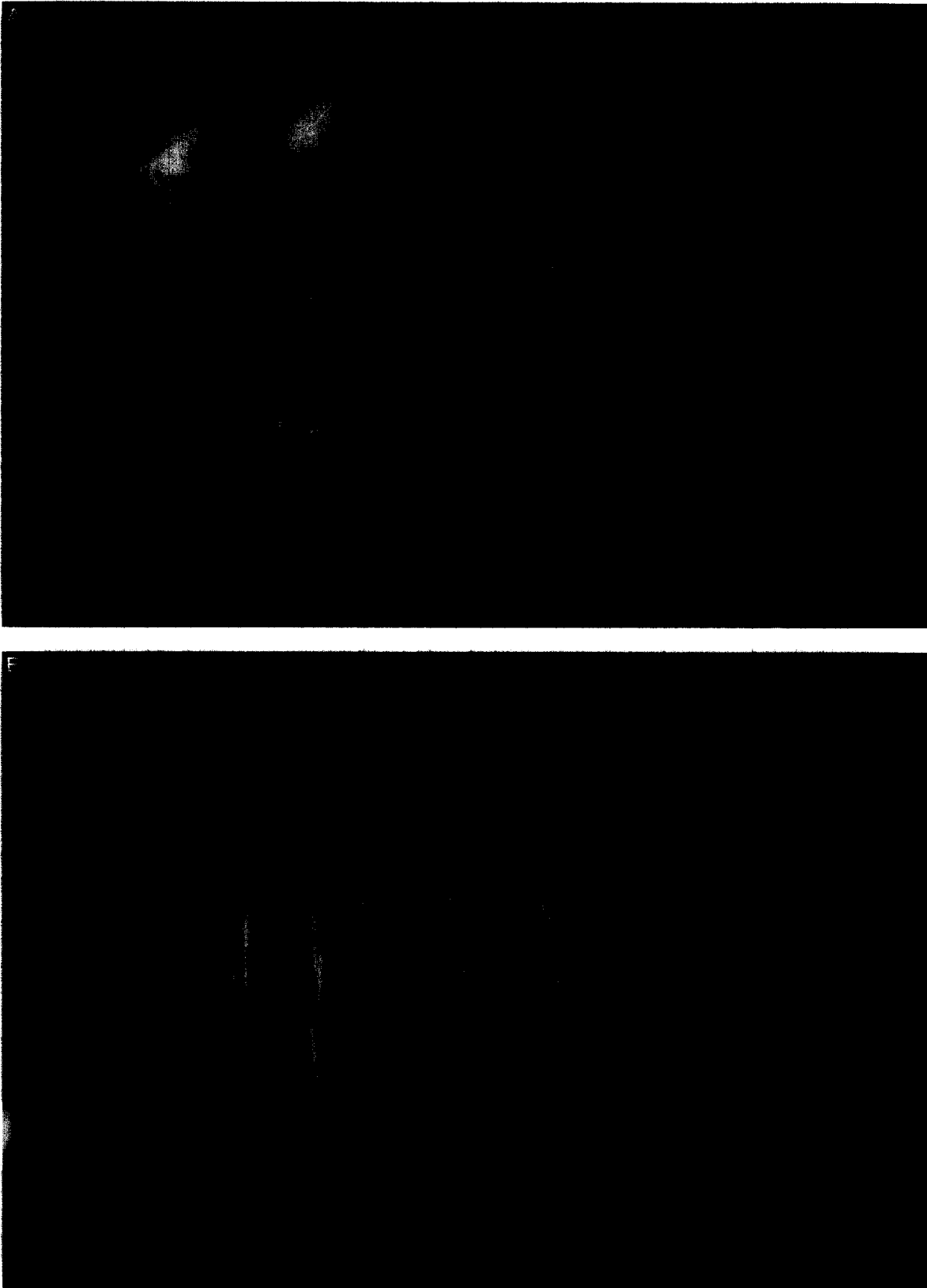


Figure 3. This young corn canopy (A) is very similar to that measured for this article. "White soil," portland cement, has just been applied to cover the natural soil. (B) Canopy of corn stems, all leaves removed, over "black soil" (furnace ash and cinders).

Table 2. Biophysical Parameters of Three Young Crop Canopies (Optical Parameters in Band 5, 0.76–0.90 μm)

Parameter	Wheat	Soybean	Corn
Leaf reflectance r_l	0.43	0.54	0.48
Leaf transmittance t_l	0.33	0.42	0.40
Soil reflectance R_s	0.073	0.715	0.053
Leaf area index LAI	1.80	1.41	8.04
Leaf angle distribution u	1.148	1.979	1.772
Leaf angle distribution v	2.646	1.363	2.569
Leaf wax refractive index k	1.35	1.35	1.45

Laboratory Apparatus

Figure 1 provides a sketch of the laboratory apparatus used for acquisition of directional measurements. The light source is a halogen arc lamp that simulates the solar spectrum, positioned above and to the side of the target. A collimating lens delivers a horizontal beam of illumination, which is directed onto the target by an optical mirror. By varying the position and angle of the mirror, the solar simulation beam can be directed at the target at any zenith angle between nadir and 45° . Power output is variable from 4000 W to 25,000 W, providing target irradiance at a value between 0.3–0.7 times the solar constant. The target is a movable stage of 1 m \times 1 m size that can be raised and lowered on an electric motor drive.

Radiance measurements are acquired by radiometers mounted on a curved frame that maintains a uniform distance of 3 m from the target. The radiometers are positioned at 10° view zenith angle increments from nadir to 90° . The frame rotates around the target on a circular track, acquiring data at 10° increments of azimuth angle. Each radiometer makes simultaneous measurements in six spectral wavebands, which are shown in Table 1. A single series of measurements thus provides 2160 observations of radiance. However, with a planar surface target such as a vegetation canopy, the field of view at ze-

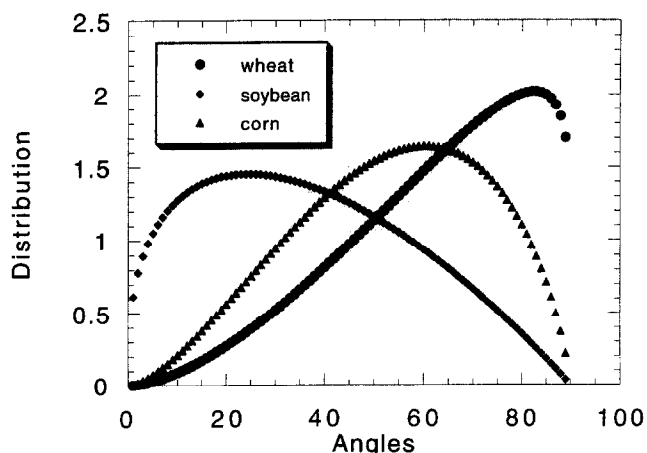
nith angles of 80° and 90° exceeds the bounds of the target. Accordingly, these measurements are normally discarded for our application, yielding datasets of 1728 measurements. Data acquisition is controlled by a micro-computer system that moves the irradiance mirror and then starts the radiometer arm assembly in motion on its circular track. Magnetic switches embedded along the track trigger the acquisition of radiometric data. A full measurement cycle requires about 10 min, which includes returning the radiometer frame to its starting position and moving the mirror to simulate a new solar zenith angle.

Calibration of the apparatus is accomplished by radiometer measurements of a barium sulfate panel, which is in turn calibrated externally using standard instruments. Panel measurements are highly repeatable. An unavoidable problem occurs when measurements are made in the backscattering direction of the principal plane—the shadow of the radiometer frame is projected onto the target. Because the taller vegetation canopies are three-dimensional targets, the shadow will interact with the canopy in a different way than when projected onto the flat panel. This effect causes some variance from a smooth angular response function for such canopies within 10° azimuth of the principal plane. Although the measured data are not as accurate in the hotspot direction because of the shadows of the frame, they are nonetheless retained. Since the sensors are very small and the frame cross section is not very large, the effect is not substantial. Electronic noise occasionally occurs in the radiometer measurements. To minimize the effects of this noise, multiple observations are normally made. The typical procedure is to repeat the measurements three times, and select the smoothest set for further processing.

Experimental Procedure

The plants comprising each canopy were grown from seed outdoors under natural conditions. They were planted in sturdy wire frame boxes measuring 0.25 m \times 1.0 m and about 0.35 m deep. The open frames permitted normal root growth. For each experiment, four boxes were placed on the target, providing a canopy with an

Figure 4. Leaf angle distribution of three canopies.



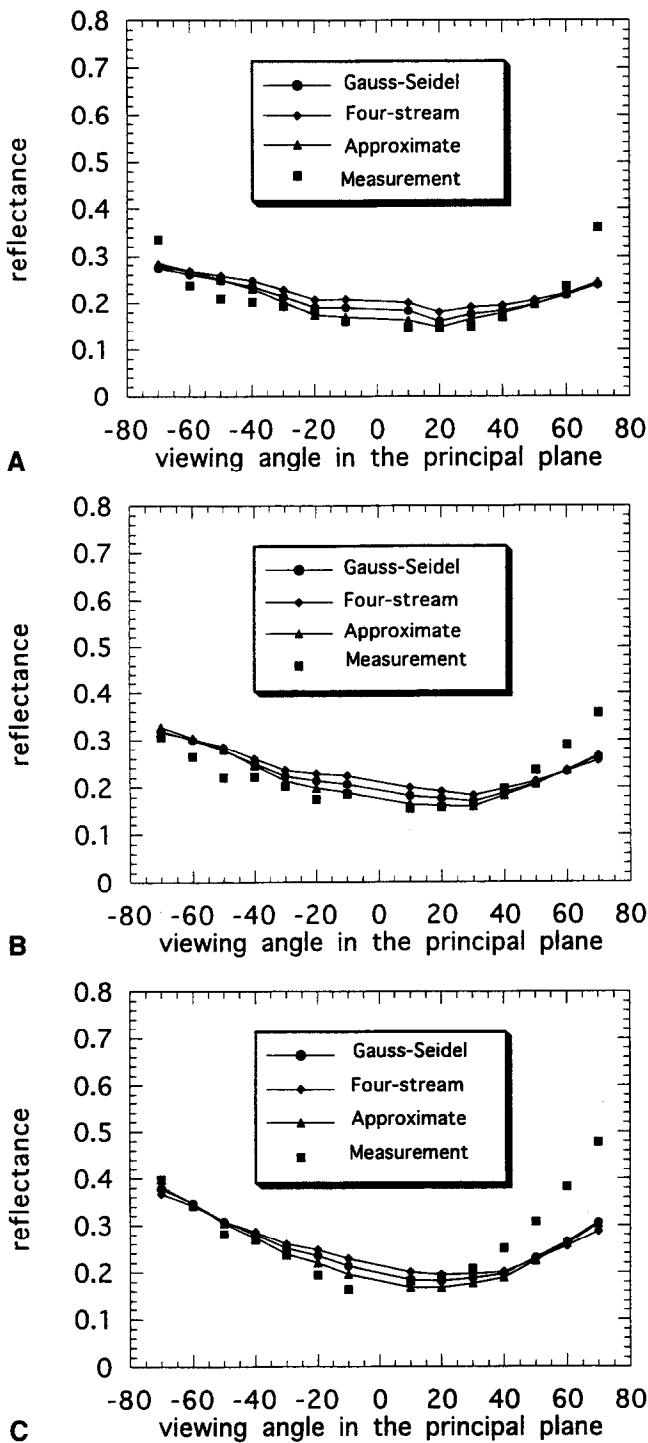


Figure 5. Comparison of observed and modeled reflectance values for a young wheat canopy in the principal plane, (A), (B), (C) 20°, 30°, and 40° illumination zenith angles, respectively. Light source at -20° , -30° , and -40° .

area of 1 m². Radiometric measurements of the canopy were then acquired at specific irradiance angles.

After radiometric measurements, each canopy was destructively sampled to determine mean leaf area, leaf height, and leaf angle distribution. Every fifth plant was

taken as a sample plant, for which the orientation of each leaf or leaflet was measured using a clinometer. Azimuthal orientation of leaves was not measured, as isotropic leaf orientation was assumed in all cases. The height of the leaf center above the canopy was also recorded. Each leaf was cut from the plant, marked with a number, and pressed between newspaper for later measurement of leaf dimensions. Where a leaf curved or abruptly changed angle, it was divided into segments and the height and angle of each segment was recorded. The segments were then cut from the leaf for determination of segment area. For plants that were not selected as samples, leaves were removed, and only the number of leaves was recorded.

Following the stripping of the leaves from the plants, another set of radiometer measurements were made to measure the reflectance of stems and soil. A final set was acquired after the stems were clipped at the soil surface and discarded. For the canopies studied, radiometric measurements of the stem canopy and the bare soil surface were not distinguishable. Figure 2 presents the measured soil bidirectional reflectance in the near-infrared band (0.76–0.9 μm). The soil was wet so that reflectance is quite low. The illumination zenith angle is 30°.

Throughout the process, panel measurements were acquired as needed. These measurements were facilitated by the movable stage, which could be lowered at any time to allow a panel to be placed above the canopy on temporary supports.

For some canopies, measurements were acquired for “white-soil” and “black-soil” backgrounds. In these cases, the soil surface was carefully spread with either portland cement (white) or furnace ash (black) before measurements were begun. While neither material created perfectly reflecting or absorbing backgrounds, they allowed exploration of the effects of light and dark soils on canopy reflectance.

CANOPY RADIATIVE TRANSFER MODELS

The one-dimensional radiative transfer equation of a horizontally homogeneous and infinite leaf canopy is given by

$$-\mu \frac{\partial I(\tau, \Omega)}{\partial \tau} + h(\tau, \Omega) G(\Omega) I(\tau, \Omega) = \frac{1}{\pi} \int_{4\pi} \Gamma(\Omega' \rightarrow \Omega) I(\tau, \Omega') d\Omega', \quad (1)$$

with the boundary conditions

$$\begin{aligned} I(0, \Omega) &= \delta(\Omega - \Omega_0) i_0, & \mu < 0, \\ I(\tau_c, \Omega) &= \frac{r_s}{\pi} \int_{2\pi} |\mu'| I(\tau_c, \Omega') d\Omega', & \mu > 0, \end{aligned} \quad (2)$$

where the unit vector Ω with an azimuth angle ϕ and a zenith angle $\theta = \cos^{-1} \mu$ with respect to the outward nor-

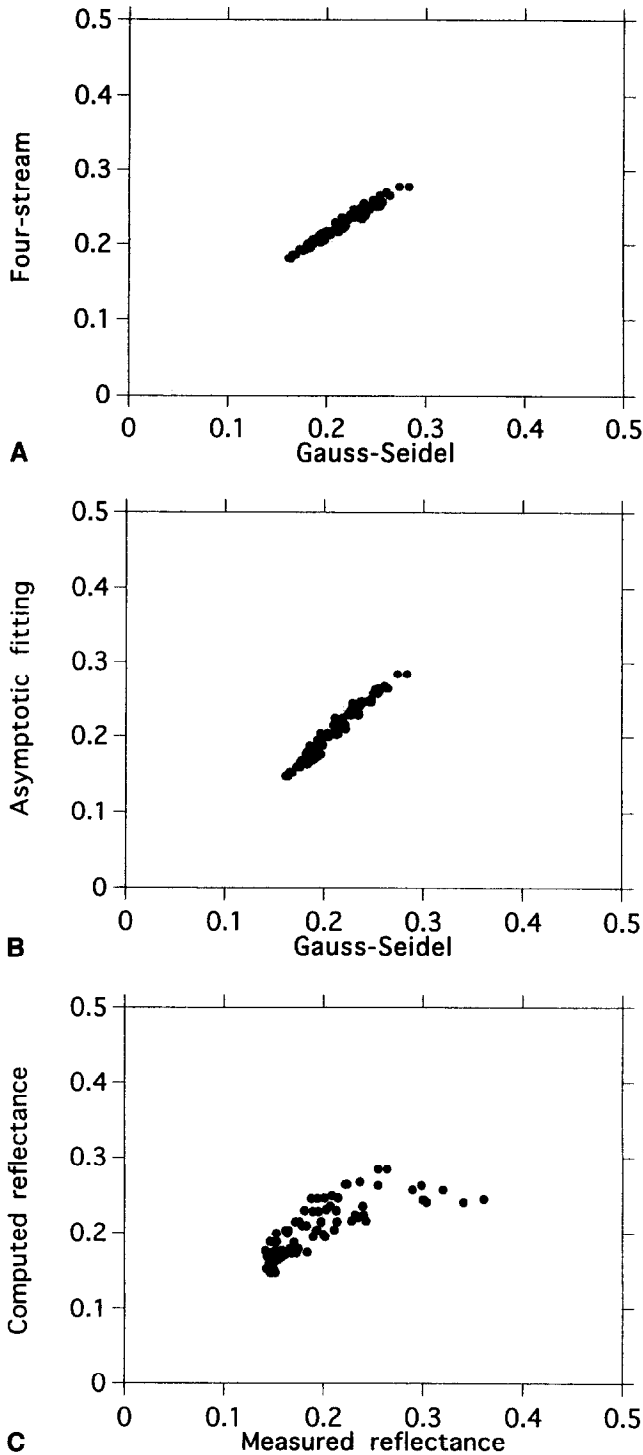


Figure 6. Comparison of observed and modeled reflectance values for a young wheat canopy in 10 azimuth angles off the principal plane with illumination angle 20° . A and B compare three models (Gauss-Seidel model, asymptotic fitting model, and four-stream model), and C compares the asymptotic fitting model with measurements.

mal characterizes the solid angle; Ω_0 characterizes the incidence direction (we will let $\mu_0 = |\mu_0|$ for simplicity); i_0 is the incidence net flux ($F_0\pi$) above the canopy; r_s is the

reflectance of a Lambertian background (e.g., soil) under the canopy; τ is the optical depth, τ_c is the optical depth of the canopy; $2\pi_-$ stands for the lower hemisphere; and $\delta(\Omega - \Omega_0)$ is the Dirac delta function for downwelling irradiance at Ω_0 .

In Eq. (1), the function $G(\Omega)$ is the mean projection of a unit foliage area in the direction Ω , the correlation function $h(\tau, \Omega)$ is used to account for the hotspot phenomenon, and the area scattering phase function $\Gamma(\Omega' \rightarrow \Omega)$ is defined as consisting of both diffuse and specular components. Detailed descriptions of these functions are provided in the literature (Marshak, 1989; Shultis and Myneni, 1988).

To solve (1), we may decompose the radiation field into three parts: unscattered radiance $I^0(\tau, \Omega)$, single-scattering radiance $I^1(\tau, \Omega)$, and multiple-scattering radiance $I^M(\tau, \Omega)$:

$$I(\tau, \Omega) = I^0(\tau, \Omega) + I^1(\tau, \Omega) + I^M(\tau, \Omega). \quad (3)$$

For the first two components, analytical solutions may be derived; they are presented in Liang and Strahler (1993a). For the multiple-scattering radiance $I^M(\tau, \Omega)$, we may write the radiative transfer equation and its boundary conditions as

$$-\mu \frac{\partial I^M(\tau, \Omega)}{\partial \tau} + G(\Omega) I^M(\tau, \Omega) = J(\tau, \Omega), \quad (4)$$

subject to boundary conditions

$$I^M(0, \Omega) = 0, \quad \mu < 0$$

$$I^M(\tau_c, \Omega) = \frac{r_s}{\pi} \int_{2\pi_-} |\mu'| [I^M(\tau_c, \Omega') + I^1(\tau_c, \Omega')] d\Omega', \quad \mu > 0$$

Here, the source function is

$$J(\tau, \Omega) = \frac{1}{\pi} \int_{4\pi} \Gamma(\Omega' \rightarrow \Omega) [I^M(\tau, \Omega') + I^1(\tau, \Omega')] d\Omega' + \frac{1}{\pi} \int_{2\pi_+} \Gamma(\Omega' \rightarrow \Omega) I^0(\tau, \Omega') d\Omega'. \quad (5)$$

As is well known, (4) is an integrodifferential equation that possesses no closed-form solution. To find a solution, two approaches are possible. First, a numerical solution may be found, typically using an iterative technique. Second, simplifying assumptions can be made that allow an analytic solution. In previous work, we have provided a numerical solution using Gauss-Seidel iteration, and two analytical solutions under differing assumptions. We briefly review these models below.

Gauss-Seidel Numerical Model

This model uses Gauss-Seidel iteration to solve the radiative transfer equation for a coupled atmosphere and canopy medium that is homogeneous in the plane (Liang and Strahler, 1993a). The medium is divided into a large number of layers, each with a small optical depth. A starting source function is specified, and the radiative

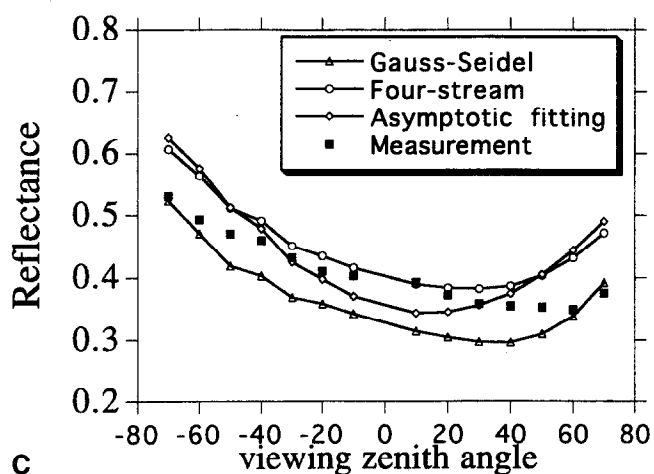
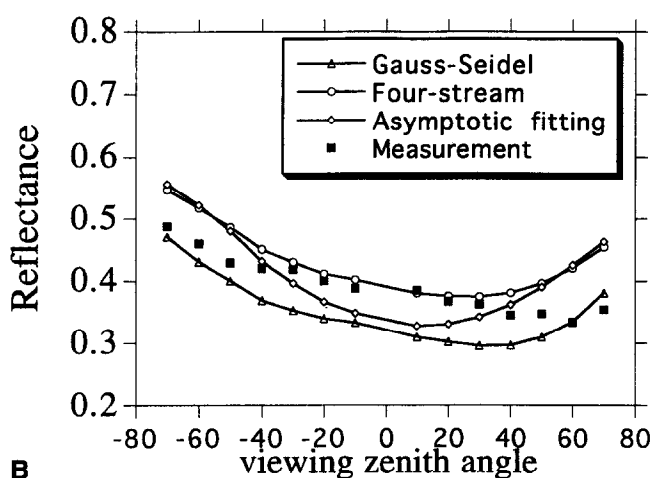
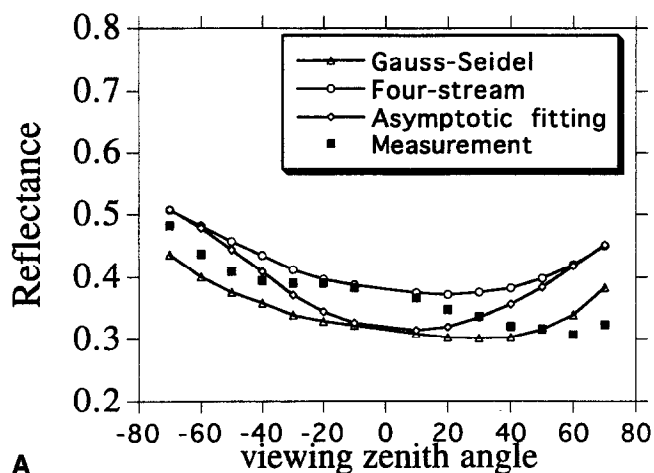


Figure 7. Comparison of observed and modeled reflectance values for a young soybean canopy. (A), (B), (C) 20°, 30°, and 40° illumination zenith angles, respectively.

transfer equation is solved in each layer successively, proceeding from the top of the atmosphere downward to the soil surface and upwards again. After each iteration, the source function is updated. Cycling continues until a stable solution is reached.

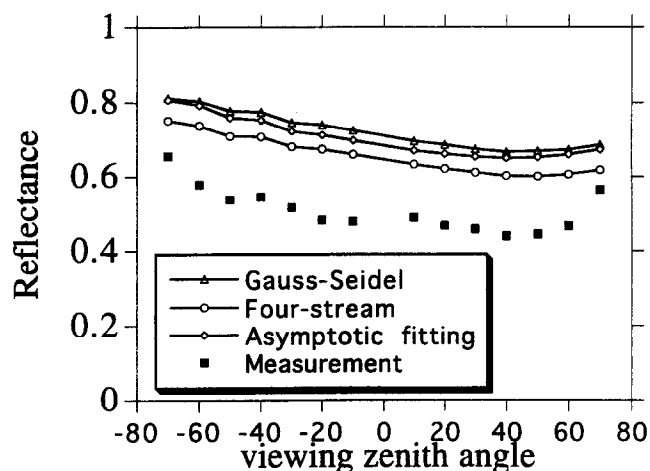


Figure 8. Comparison of observed and modeled reflectance values for a young soybean canopy with white soil background. The illumination zenith angle is 40°.

Asymptotic Fitting Model

The asymptotic fitting model (Liang and Strahler, 1993b) uses the well-known solution of Van de Hulst (1980) to the radiative transfer equation for a semiinfinite medium with an arbitrary phase function. It is modified for soil reflectance using a relation from King (1987). The model used in this article departs slightly from that published earlier (Liang and Strahler, 1993b) in that an empirical relationship is used to derive the Henyey–Greenstein asymmetry parameter from an empirical relationship with biophysical parameters, as described in Liang and Strahler (1995).

Four-Stream Model

In the four-stream model, an analytical solution is derived for a coupled plane-parallel atmosphere–canopy medium in which the radiation field is restricted to four streams (Liang and Strahler, 1995). The four streams are taken at Gaussian quadrature points. As in the Gauss–Seidel iterative model, we invoke only the canopy portion of the model under conditions of direct beam irradiance.

DATA ANALYSIS

Although more extensive analyses of reflectance measurements acquired at the Solar Simulation Laboratory have been made, we report here only a limited set that is selected for validation of the three candidate models described above. Since the three models differ primarily in how they approximate multiple scattering, we present only data and model runs from the near-infrared (Band 5, Table 1) where multiple scattering within the leaf canopy will be large. Due to a detector malfunction, data acquired by the nadir-viewing radiometer in this band were not available.

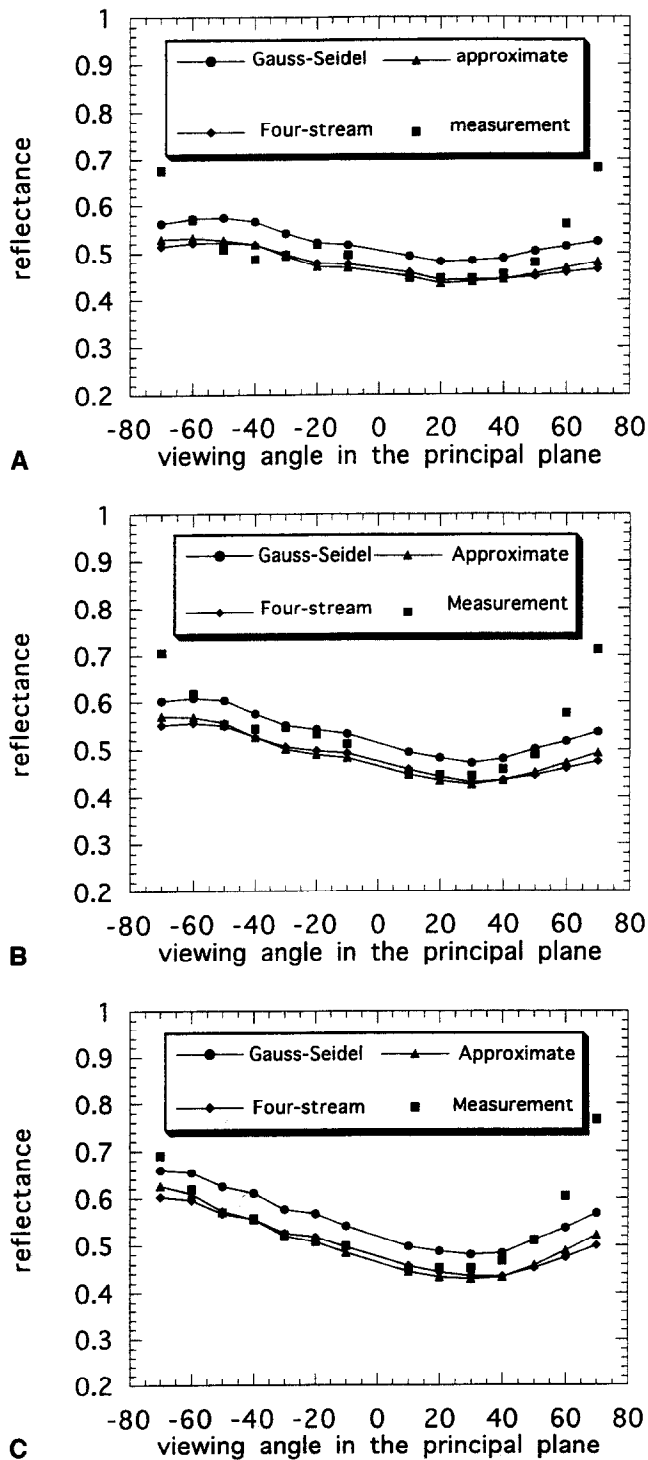


Figure 9. Comparison of observed and modeled reflectance values for a young corn canopy. A, B, C) 20°, 30°, and 40° illumination zenith angles, respectively.

Note also that for these model runs we have assumed isotropic soil reflectance with a value integrated from bare-surface observations. This is because the asymptotic model does not provide for an anisotropically reflecting surface layer. Using an isotropic lower bound

for all three models allows them to be compared more directly.

Results are presented for three crop canopies: wheat, soybean, and corn. Figure 3 shows a young corn canopy at the Solar Simulation Laboratory very similar to that measured for this paper. Table 2 provides a list of the biophysical parameters used in the model runs. Leaf reflectance and transmittance were determined by a spectrometer providing monochromatic illumination and measurement at fixed angles. An apparatus utilizing an integrating sphere was not available. In the near-infrared band, however, the sum of the measured leaf reflectance and transmittance was larger than 1. As a result, we lowered the leaf reflectance and transmittance by 15% to match typical values in the literature. The leaf angle distributions of three canopies are presented in Figure 4. They are fit by a two-parameter beta distribution (Goel and Strelbel, 1984) with values as shown in Table 2. Three soil reflectances correspond to three conditions: black soil, white soil, and natural soil, respectively.

Wheat Canopy

For the wheat canopy, shown in Figure 5, all three models predict more-or-less similar angular reflectances, although there is some significant difference among them in the nadir portion of the scan. (In all figures presented in this article, "approximate" denotes the asymptotic fitting model.) The young canopy, consisting of shoots with largely vertical leaves, shows a reasonably good fit to the models especially at smaller view zenith angles. However, as illumination angle increases, the canopy shows an increasing brightness trend in the forward scattering direction that is not predicted by the models. We may speculate that the discrepancy is due to the assumption of isotropic soil reflectance, since the soil appeared to the observer at the time of measurement to have an enhanced brightness in the forward scattering direction (Fig. 2). The detailed discussions of soil effects on canopy directional reflectance can be found elsewhere (Huete, 1989).

It will be interesting to examine the differences of these three models and measurements in other azimuthal planes given the specific canopy configuration and optical parameters. Figure 6 compares the reflectance between model calculations and measurement at several azimuth planes. The illumination zenith angle is 20°. There are 10 azimuth angles in this figure, ranging from 30° to 330°. Each two azimuth angles have 14 points, as shown in the previous figures. The three model calculations (A, B) are almost identical, but there exists some scatter between asymptotic fitting model calculations and actual measurements (C).

Soybean Canopy

The soybean canopy consisted of relatively small plants and exhibited a leaf area index of only 1.41. Significant

row effects were still visible, so the canopy was arranged with the principal plane across the rows.

Figure 7 compares the model calculations with measurements for this soybean canopy. The difference between model calculations and measurements is probably because of the inhomogeneous canopy field. The four-stream approximation produces a very similar angular pattern to that produced by the Gauss-Seidel algorithm, although the relative difference is as large as about 20%.

Reflectance measurements of this canopy (Fig. 8) were also made with one "white soil" background, which enhanced multiple scattering considerably. The general pattern of the graphs shows all models predicting reflectance values significantly larger than the measured reflectances. We believe that measurements of canopy reflectance are artificially low for this canopy due to the finite extent of the canopy. Because the canopy departs significantly from a two-dimensional surface, light is lost from the sides of the canopy and is not scattered back into the target portion as it would be for a canopy of greater areal extent. The effect is to reduce the radiance emerging from the canopy to levels lower than those predicted by the analytical models. Allowing for this effect, the general shape of the distribution of models as a function of zenith angle follows the measurements quite well.

Corn Canopy

The corn canopy consisted of taller, closely spaced plants over a natural soil background. They were about 2 months old, 1.2 m tall, and exhibited a leaf area index of about 8. At this LAI, multiple scattering is very strong, and we see some of the same effects as in the soybean canopy (Fig. 9). That is, the Gauss-Seidel solution shows a higher reflectance than the two approximation methods, and the measured canopy reflectance is somewhat lower due to the escape of scattered radiation from the sides of the canopy.

In general, the shape of the observed reflectance curve matches the models well at low and intermediate zenith angles. However, canopy reflectance increases sharply at the extremes. One reason might be specular reflectance by the many nearly horizontal leaf segments. Specular effects could exceed those modeled if the parameter k (leaf wax refractive index), chosen from the literature, was too small. Another possible error lies in the geometry of the field of view of the radiometers. At 60° and 70° view angles, small portions of the field of view at near and far edges may fall outside of the calibration panel. However, with a deep canopy such as that of corn, the near field of view is likely to be completely occupied by leaves from the side of the canopy. Thus, the enhanced reflectance may be a result of normalizing by a panel reading that is too small for the target. This would not be as much of a problem for a shorter canopy, such as those of young wheat or soybean, which would

conform better to the field of view of the calibration panel.

DISCUSSION

The canopy reflectance measurements in the near-infrared band acquired at the Solar Simulation Laboratory were compared with the radiative transfer models for describing the angular reflectance of plane-parallel leaf canopies. Closest agreement between model and measurement occurs for the young wheat canopy, which has a moderate leaf area index, dark (normal) soil, and is not very tall in relation to the width of the target. Under these conditions, measurements are most accurate and model assumptions tend to approach reality.

For the soybean and corn canopies, departures of measurements from models are noted that are related to the finite nature of the canopy sample and its interaction with the field of view of the radiometers. The former problem is most obvious in the case of the soybean canopy on white soil, where a significant proportion of the multiply scattered radiation appears to be lost through the sides of the canopy, decreasing upwelling radiance by about one-third.

The corn canopy, which has a high leaf area index and is almost half as tall as the width of the target stage, shows strongly increasing reflectance at high view zenith angles apparently due to field of view effects. One way to reduce these effects is simply to narrow the instantaneous field of view. However, this reduces the signal-to-noise ratio and makes the problem of aligning the radiometers to the same target field of view more difficult. Further, normal irregularities in the canopy will loom larger in the field of view, adding additional variance. These trade-offs need to be examined for future measurement programs.

An alternative is to model the canopy as three-dimensional—that is, as an isolated rectangular block of scattering material. Some general three-dimensional canopy radiative transfer models already exist (e.g., Myneni et al., 1990b). However, to capture exiting radiance from the entire block, the size of the canopy would need to be reduced, or else the field of view of the radiometers increased.

The comparison of model results for the cases posed by these three canopies points out the importance of the treatment of multiple scattering in near-infrared canopy reflectance. Both the asymptotic and four-stream models diverge significantly from the Gauss-Seidel iterative model for two of the three cases, showing that their approximations can be limiting, especially in the extreme case of white soil.

This work was supported in part by the National Aeronautics and Space Administration under Grant NAGW-2082, Contracts NAS5-30917 and NAS5-31369, the U.S. National Science Foun-

dition under Grant INT-9014263, and the National Science Foundation of China under Grant 49171052.

REFERENCES

- Deering, D. W., Middleton, E. M., and Eck, T. F. (1994), Reflectance anisotropy for a spruce-hemlock forest canopy. *Remote Sens. Environ.* 47:242-260.
- Goel, N. S. (1988), Models of vegetation canopy reflectance and their use in estimation of biophysical parameters from reflectance data. *Remote Sens. Rev.* 4:1-222.
- Goel, N. S., and Strebel, D. E., (1984), Simple beta distribution representation of leaf orientation in vegetation canopies. *Agron. J.* 76:800-803.
- Huete, A. R. (1989), Soil influences in remotely sensed vegetation-canopy spectra. In *Theory and Applications of Optical Remote Sensing* (G. Asrar, Ed.), Wiley, New York, pp. 107-141.
- Huete, A. R., and Jackson, R. D. (1988), Soil and atmosphere influences on the spectra of partial canopies. *Remote Sens. Environ.* 25:89-105.
- Huete, A. R., Jackson, R. D., and Post, D. F. (1985), Spectral response of a plant canopy with different soil backgrounds. *Remote Sens. Environ.* 17:37-53.
- Irons, J. R., Campbell, G. S., Norman, J. M., Graham, D. W., and Kovalick, W. M. (1992), Prediction and measurement of soil bidirectional reflectance. *IEEE Trans. Geosci. Remote Sens.* 30:249-260.
- Kimes, D. S., Newcomb, W. W., Schutt, J. B., Pinter, P. J., Jr., and Jackson, R. D. (1984), Directional reflectance factor distributions of a cotton row crop. *Int. J. Remote Sens.* 5:263-277.
- King, M. D. (1987), Determination of the scaled optical thickness of clouds from reflected solar radiation measurements. *J. Atmos. Sci.* 44:1734-1751.
- Li, X., and Strahler, A. H. (1986), Geometric-optical bidirectional reflectance modeling of a conifer forest canopy. *IEEE Trans. Geosci. Remote Sens.* 24:906-919.
- Li, X., and Strahler, A. H. (1992), Geometric-optical bidirectional reflectance modeling of the discrete-crown vegetation canopy: effect of crown shape and mutual shadowing. *IEEE Trans. Geosci. Remote Sens.* 30:276-292.
- Liang, S., and Strahler, A. H. (1993a), Calculation of the angular radiance distribution for a coupled atmosphere and canopy. *IEEE Trans. Geosci. Remote Sens.* 31:491-502.
- Liang, S., and Strahler, A. H. (1993b), An analytic BRDF model of canopy radiative transfer and its inversion. *IEEE Trans. Geosci. Remote Sens.* 31:1081-1092.
- Liang, S., and Strahler, A. H. (1995), An analytic radiative transfer model for the coupled atmosphere and canopy. *J. Geophys. Res.* 100:5085-5094.
- Marshak, A. L. (1989), The effect of the hot spot on the transport equation in plant canopies. *J. Quant. Spectrosc. Radiat. Transfer* 42:615-630.
- Myneni, R. B., Ross, J., and Asrar, G. (1990a), A review on the theory of photon transport in leaf canopies. *Agric. For. Meteorol.* 45:1-153.
- Myneni, R. B., Asrar, G., and Gerstl, S. A. W. (1990b), Radiative transfer in three-dimensional leaf canopies. *Transport Theory Stat. Phys.* 19:205-250.
- Ranson, K. J., Biehl, L. L., and Bauer, M. E. (1985a), Variation in spectral response of soybeans with respect to illumination, view and canopy geometry. *Int. J. Remote Sens.* 6:1827-1842.
- Ranson, K. J., Daughtry, C. S. T., Biehl, L. L., and Bauer, M. E. (1985b), Sun-view angle effects on reflectance factors of corn canopies. *Remote Sens. Environ.* 18:147-161.
- Shultis, J. K., and Myneni, R. B. (1988), Radiative transfer in vegetation canopies with an isotropic scattering. *J. Quant. Spectrosc. Radiat. Transfer* 39:15-129.
- Suits, G. W. (1972), The calculation of the directional reflectance of a vegetative canopy. *Remote Sens. Environ.* 2:117-125.
- Van de Hulst, H. C. (1980), *Multiple Light Scattering, Tables, Formulas and Applications*, Vols. 1 and 2, Academic, New York, 739 pp.
- Vanderbilt, C. L., and Grant, L. (1986), Polarization photometer to measurement bidirectional reflectance factor R (55°, 0°; 55°, 180°) of leaves. *Opt. Eng.* 25:566-571.